

*A comparative analysis of the attribution of extreme summer precipitation in south and north parts of the East China monsoon region—with the year 2020 as an example*

Article

Accepted Version

Li, R., Liu, X., Xu, Y. and Dong, B. ORCID:  
<https://orcid.org/0000-0003-0809-7911> (2023) A comparative analysis of the attribution of extreme summer precipitation in south and north parts of the East China monsoon region—with the year 2020 as an example. *International Journal of Climatology*, 43 (15). pp. 7199-7217. ISSN 0899-8418 doi:  
<https://doi.org/10.1002/joc.8260> Available at  
<https://centaur.reading.ac.uk/113500/>

It is advisable to refer to the publisher's version if you intend to cite from the work. See [Guidance on citing](#).

To link to this article DOI: <http://dx.doi.org/10.1002/joc.8260>

Publisher: Wiley

All outputs in CentAUR are protected by Intellectual Property Rights law, including copyright law. Copyright and IPR is retained by the creators or other copyright holders. Terms and conditions for use of this material are defined in the [End User Agreement](#).

[www.reading.ac.uk/centaur](http://www.reading.ac.uk/centaur)

**CentAUR**

Central Archive at the University of Reading

Reading's research outputs online

1 **A comparative analysis of the attribution of extreme summer precipitation in south**  
2 **and north parts of the East China monsoon region - with the year 2020 as an**  
3 **example**

4  
5 Rouke Li <sup>a, b, c</sup>, Xiaodong Liu <sup>a, b</sup>, Ying Xu<sup>c</sup>, Buwen Dong<sup>d</sup>

6  
7 <sup>a</sup> State Key Laboratory of Loess and Quaternary Geology, Institute of Earth  
8 Environment, Chinese Academy of Sciences, Xi'an, 710061, China

9 <sup>b</sup> University of Chinese Academy of Sciences, Beijing, 100049, China

10 <sup>c</sup> National Climate Center, Beijing, 100081, China

11 <sup>d</sup> National Centre for Atmospheric Science, Department of Meteorology, University of  
12 Reading, Reading, United Kingdom

13  
14 **Correspondence**

15 Rouke Li and Xiaodong Liu, State Key Laboratory of Loess and Quaternary Geology,  
16 Institute of Earth Environment, Chinese Academy of Sciences, Xi'an, 710061, China.

17 Email: lirk4321@163.com (R.L.) and liuxd@loess.llqg.ac.cn (X.L.)

18  
19 **Funding information**

20 National Natural Science Foundation of China, Grant/Award Numbers: 41991254;  
21 China Three Gorges Corporation, Grant/Award Numbers: 0704081; key Youth  
22 Innovation Team of China Meteorological Administration, Grant/Award Numbers:  
23 CMA2023QN15.

24  
25 **Abstract**

26 In summer 2020, several watersheds in China monsoon region experienced  
27 historically unusually heavy precipitation. The flooding associated with these heavy  
28 precipitation events led to devastating impacts on human life, infrastructure, agriculture,

1 and economy. Using historical climate simulations from the HadGEM3-GA6 and  
2 CMIP6 models under influences of natural and/or anthropogenic forcings, we conducted  
3 a comparative study on the attribution of extremely heavy precipitation events in  
4 summer 2020 in the mid-lower reaches of the Yangtze River and the mid-lower reaches  
5 of the Yellow River- Hai River Basin which locates respectively in the south and north  
6 parts of the East China monsoon region. The potential contributions of anthropogenic  
7 forcings to monthly-scale extreme precipitation and daily maximum precipitation  
8 (RX1day) were examined. The results suggest that human activities have decreased the  
9 probability of month-scale extreme precipitation events in south part of the East China  
10 monsoon region. For RX1day extreme precipitation events, anthropogenic factors have  
11 increased their probability in both regions. However, the influence of anthropogenic  
12 forcings on month-scale extreme precipitation events in north part of the East China  
13 monsoon region is not robust among two attribution systems. Further analyses indicated  
14 that anthropogenic aerosols (AER) make both month-scale extreme precipitation events  
15 and extreme RX1day less likely to occur in summer 2020, and greenhouse gases (GHG)  
16 increase the likelihood of both. GHG influences on Rx1day overwhelm AER influences,  
17 leading to an increase of the probability of Rx1day similar to the 2020 events in both  
18 regions. In contrast, the decrease of the probability of month-scale precipitation in south  
19 part of the East China monsoon region is predominantly due to aerosol forcing. The  
20 model projections show that the likelihood of both monthly and daily extreme  
21 precipitation events in both regions will increase in the future. Accordingly, the  
22 recurrence period of extreme precipitation events will be shortened by the end of the  
23 21st century, which is more significant under the high emission scenario.

24

## 25 **KEYWORDS**

26 East China monsoon region, extreme precipitation, attribution, future projection

27

## 28 **1 INTRODUCTION**

1        Since the industrial revolution, the global mean near-surface temperature has  
2 increased by about 1.10°C (0.97-1.25°C), resulting in multiple impacts on other climate  
3 system components, including increasingly frequent extreme weather events (IPCC,  
4 2021). Observational studies suggest a strong link between climate warming and  
5 increased extreme precipitation at the global scale (Papalexiou and Montanari, 2019).  
6 Furthermore, extreme precipitation events have increased in many parts of China (Wang  
7 and Qian, 2009). Persistent heavy precipitation events that were anomalously greater  
8 than normal during the summer 2020 resulted in record-breaking precipitation in the  
9 Yangtze River catchment and the Yellow River catchment (China Meteorological  
10 Administration, 2021). According to the Ministry of Emergency Management (2021),  
11 floods caused by continuous precipitation in July 2020 affected 38.173 million people,  
12 and 3,868.7 thousand hectares of crops, and resulted in 109.74 billion yuan in direct  
13 economic losses; in August, 41.35 billion yuan in direct economic losses occurred.

14        In recent years, an increasing number of studies have linked increased precipitation  
15 extremes to human activities. Human activities have caused global changes in terrestrial  
16 precipitation (IPCC, 2021). By enhancing the water cycle, anthropogenic warming may  
17 influence mean and extreme precipitation (He and Soden, 2015; Li et al., 2021b; Tao et  
18 al., 2016; Vecchi et al., 2006; Wu et al., 2022). 2/3 of the land area of the Northern  
19 Hemisphere has experienced enhanced extreme precipitation, and multi-model  
20 simulations of precipitation response to anthropogenic forcing are consistent with  
21 changes in terrestrial extreme precipitation observed in the Northern Hemisphere (Min  
22 et al., 2011; Zhang et al., 2013). The more extreme the precipitation event, the clearer  
23 the anthropogenic influence (Wang et al., 2023). The human influence dominated by the  
24 GHG effect has intensified extreme precipitation, especially in continental and regional  
25 extreme precipitation (Chen and Sun, 2017; Dong et al., 2021; Kirchmeier-Young and  
26 Zhang, 2020; Sun et al., 2021; Xu et al., 2022). For the 2020 extreme precipitation,  
27 anthropogenic forcing has decreased the likelihood of the month-scale extreme rainfall  
28 that was observed in the lower Yangtze River in 2020 (Zhou et al., 2021; Lu et al., 2022;

1 Ma et al., 2022; Tang et al., 2022). However, the influence of anthropogenic forcing on  
2 RX1day over YZR, month-scale precipitation and RX1day over HHB regions in 2020  
3 has received less attention.

4 Additionally, human activities may increase the probability of short-term heavy  
5 precipitation and decrease the frequency of long-term precipitation in China (Lu et al.,  
6 2020; Zhang et al., 2020). However, different studies defined events in different regions  
7 and the study areas are fragmented, leading to different conclusions (Stott et al., 2016).  
8 It has been suggested that human activities may have increased the risk of long-term  
9 persistent and short-term extreme precipitation in the Yangtze River basin and southern  
10 China (Sun and Miao, 2018; Sun et al., 2019; Yuan et al., 2018; Zhou et al., 2018).  
11 However, some scholars thought that human activities had reduced the risk of long-term  
12 precipitation in south of the Yangtze River and in southern China, increasing the risk of  
13 drought in early summer in Yunnan (Li et al., 2018; Li et al., 2021a; Lu et al., 2020;  
14 Nanding et al., 2020;). The reduced flood risks in west-central China may also be  
15 related to human activities (Ji et al., 2020; Zhang et al., 2020). Considering that the  
16 above studies involve different regions and time periods, it is difficult to make regional  
17 comparisons.

18 Greenhouse gases (GHG) and aerosols (AER) emissions are the two most  
19 important anthropogenic climate-forcing factors. Increases in GHG have contributed to  
20 the observed intensification of extreme precipitation over many land areas (Chen and  
21 Sun 2017; Dong et al. 2020, 2021; Lu et al. 2020), resulting from enhanced atmospheric  
22 water-holding capacity by GHG induced warming (Min et al. 2011; Zhang et al. 2013;  
23 Myhre et al., 2014; Lin et al. 2018;). AER can affect local climate directly by radiative  
24 absorption and scattering and indirectly by changing cloud characteristics like albedo  
25 and lifetime through their role as cloud condensation nuclei (Boucher et al. 2013;  
26 Bellouin et al., 2020). Some recent studies have demonstrated that increased AER  
27 emissions during the last few decades have played an important role in the observed  
28 weakening of the East Asian summer monsoon circulation (Polson et al., 2014; Dong et

1 al. 2020; Song et al. 2014; Chen et al., 2018; Tian et al. 2018; Diao et al., 2021) and the  
2 reduced summer extreme precipitation over north China (Lin et al. 2018; Zhang et al.  
3 2017; Guo et al. 2023). In addition to anthropogenic influences, strong natural  
4 variability is still nonnegligible in regulating regional precipitation extremes (Li et al.,  
5 2021a; Martel et al., 2018).

6 At the end of the 21st century, as global warming increases, the Asian monsoon  
7 region will become increasingly warm and wet, and sudden-onset floods such as urban  
8 rainfalls and flash floods, which are strongly associated with extreme precipitation, will  
9 become more frequent and severe (IPCC, 2021; Kharin et al., 2013; O'Gorman, 2012).  
10 GHG-induced warming will increase extreme precipitation significantly (Min et al.,  
11 2011; Myhre et al., 2014), while anthropogenic aerosol emission reductions will  
12 exacerbate extreme precipitation in East Asia (Lin et al., 2018; Myhre et al., 2014;  
13 Rotstayn et al., 2013; Wang et al., 2015; Xu et al., 2018; Zhao et al., 2019). The  
14 combination of the two could make extreme precipitation significantly more intense in  
15 the context of future warming. Thus, it is of great interest to quantify the risk of summer  
16 2020-like extreme heavy precipitation events over China in future.

17 This paper analyzes heavy precipitation events in the summer 2020 in two regions  
18 over East China, namely the mid-lower reaches of the Yangtze River (YZR), the  
19 mid-lower reaches of the Yellow River- Hai River basin (HHB).

20 The main aims of the study are to assess the anthropogenic influences on the  
21 likelihood of heavy precipitation events in summer 2020 in two regions over East China  
22 using the Met Office HadGEM3-GA6 attribution system (Ciavarella et al. 2018) and the  
23 sixth phase of Coupled Model Inter-comparison Project (CMIP6) (Eyring et al. 2016;  
24 Gillett et al. 2016). In addition, the probability of summer 2020-like extreme  
25 precipitation events under different shared socioeconomic paths are projected and  
26 quantified.

27 The rest of the paper is organized as follows: in Section 2, observational and model  
28 data, as well as their analysis methods, are described. The simulated precipitation and

1 precipitation extremes in summer over China are evaluated in Section 3. Section 4  
2 focuses on the attribution of observed events, and Section 5 documents projected changes.  
3 The conclusion is given in Section 6.

## 4 5 **2 DATA AND METHODS**

### 6 **2.1 Data**

7 In this study, we used quality-controlled daily rainfall station data provided by the  
8 National Meteorological Information Center (NMIC) of China from over 2400  
9 meteorological stations during 1961-2020. Cressman interpolation (Cressman, 1959)  
10 was used to interpolate the original station observations data to  $0.56^\circ \times 0.83^\circ$  (the same  
11 as the HadGEM3-GA6 model resolution).

12 For the study period, atmospheric circulation conditions were analyzed using the  
13 global reanalysis dataset from the National Centers for Environmental Prediction  
14 (NCEP) and the National Center for the Atmosphere (NCAR) (Kalnay et al., 1996). The  
15 reanalysis data of the variables of geopotential height, temperature, precipitable water,  
16 sea level pressure, specific humidity, zonal and meridional winds were used, with a  
17 spatial resolution of  $2.5^\circ \times 2.5^\circ$ , a temporal resolution of days, and a vertical resolution  
18 of 17 layers for 3-dimension variables.

19 Based on the HadGEM3-GA6 model developed by Hadley Center (Ciavarella et al.,  
20 2018), with N216 resolution of  $0.56^\circ \times 0.83^\circ$ , this study examined the effects of  
21 anthropogenic forcings of 2020-like monthly-scale and daily extreme precipitation in  
22 two regions over East China. The model simulations include two sets of ensemble  
23 simulations. One set is ALL-forced (historical) simulations that are conditioned on  
24 observed sea surface temperatures (SST) and sea ice (HadISST) (Rayner et al., 2003).  
25 The other set is natural forced (historicalNat) simulations in which anthropogenic  
26 signals from observed SST are removed with preindustrial forcings. Both historical and  
27 historicalNat ensembles have 15 members in the historical period (1961-2013) and 525  
28 members in 2020. Therefore, the occurrence probabilities and the resulting attribution



1 conclusions are conditioned on the 2020 SST and sea ice.

2 To further validate the attribution conclusions, we used simulations from climate  
3 models that participated in the Coupled Model Intercomparison Project Phase 6 (CMIP6)  
4 and in Detection and Attribution Model Intercomparison Project (DAMIP) (Eyring et al.  
5 2016; Gillett et al. 2016) under all anthropogenic and natural forcing combined (ALL),  
6 and natural forcing (NAT) with a set of 12 different climate models. Details of the  
7 models are given in Table 1 and Table S1. Since the coupled simulations have an  
8 evolving SST and sea ice, we chose the years 2011-2020, which are closest to 2020,  
9 using the SSP5-8.5 (Shared Socioeconomic Pathway 5/Representative Concentration  
10 Pathway 8.5, O'Neill, et al., 2016) to extend CMIP6 ALL simulations from 2014 to  
11 2020, to represent the current climate. We consider all members in CMIP6 ALL and  
12 NAT simulations for the decade 2011-2020 as an ensemble. Taking month-scale  
13 precipitation over YZR as an example, there are 750 samples in the CMIP6 ALL  
14 ensemble (75 simulations multiplied by 10 years) and 570 samples in NAT ensembles,  
15 respectively. It is worth noting that, unlike the 2020 SST-based HadGEM3-GA6 model,  
16 the CMIP6 simulations cover a wide range of ocean states. Therefore, the event  
17 probabilities estimated below are differently conditioned, and the two datasets'  
18 attribution results will not be directly comparable.

19 In addition, simulations of the same set climate models (see Table S1) from the  
20 CMIP6 in the Scenario Model Comparison Program (ScenarioMIP, O'Neill, et al., 2016)  
21 were selected for the SSP2-4.5, SSP3-7.0, and SSP5-8.5 scenarios for 2081-2100 and  
22 these model simulations were used to assess the probability of the occurrence of  
23 summer 2020-like extreme precipitation events over China at the end of the  
24 21st-century.

25 To reduce differences between models and observations, making the results more  
26 accurate, we perform a linear-scaling bias correction to the model simulations.  
27 Precipitation and RX1day are corrected with a factor based on the ratio of long-term  
28 monthly mean observed and simulated data during 1961-2010 (Teutschbein and Seibert,

1 2012).

2 For station data, we first calculated month-scale precipitation (or RX1day), and  
3 then calculated precipitation anomalies (or RX1day percentage anomalies) relative to  
4 1961-2010 average at each station. To prevent errors in sparsely populated areas of  
5 stations, we used Cressman interpolation to interpolate RX1day and monthly  
6 precipitation station data to model resolution, and finally got the regional average of  
7 RX1day or monthly precipitation using area-weighted mean. For simulated data, we  
8 first calculated the indices at each grid on the original grid of each model then  
9 calculated the regional average to prevent errors during the interpolation process for  
10 simulated data. To remove model bias, monthly precipitation anomalies and RX1day  
11 percentage anomalies have been calculated using the 1961-2010 climatology. Details of  
12 the indices calculation process could be found in the Supplementary information.

13 TABLE 1 Overview of the 12 CMIP6 global climate models

CMIP6 Model	Country	CMIP6 Model	Country
ACCESS-CM2	Australia	IPSL-CM6A-LR	France
ACCESS-ESM1-5	Australia	MIROC6	Japan
BCC-CSM2-MR	China	CESM2	United States
CanESM5	Canada	FGOALS-g3	China
CNRM-CM6-1	France	MRI-ESM2-0	Japan
HadGEM3-GC31-LL	United Kingdom	NorESM2-LM	Norway

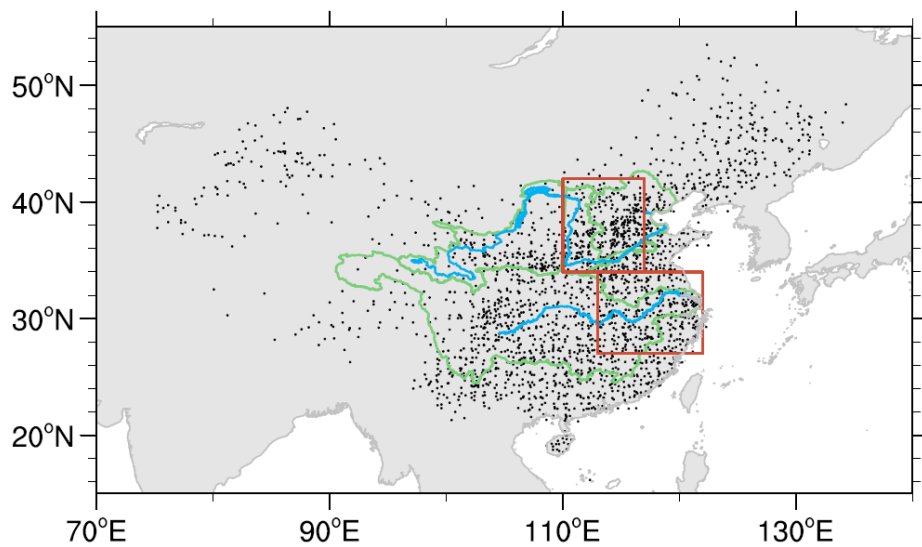
14

## 15 **2.2 Methods**

### 16 2.2.1 Selection of the study area

17 In summer (June-July-August) 2020, China had 14.7% more precipitation than  
18 normal, which is the second heaviest since 1961 (China Meteorological Administration,  
19 2021). Flooding rainfall was mainly concentrated in the mid-lower reaches of the  
20 Yangtze River, with a 62-day-long plum rainy season and the heaviest plum rain since  
21 1961. A total of 21 numbered floods occurred in major rivers such as the Yangtze,

1 Yellow, and Huai Rivers (Ministry of Emergency Management, 2021). To investigate  
2 the contribution of anthropogenic impacts to extreme precipitation events in these  
3 regions over East China, respectively, this paper selects YZR and HHB regions where  
4 stations are densely distributed, as representative regions in south and north parts of the  
5 East China, respectively, for the summer 2020-like extreme precipitation events. The  
6 two study regions are shown in red boxes in Figure 1.



7  
8 FIGURE 1 Study regions and distribution of weather stations used. Dots are stations of observations.  
9 Green lines highlight the Yangtze River basin, the Yellow River basin and Hai River basin. Red  
10 boxes highlight the study area of the mid-lower reaches of the Yangtze River (27~34°N, 113~122°E,  
11 YZR region), and the mid-lower reaches of the Yellow River- Hai River basin (34~42°N, 110~117°E,  
12 HHB region).

13

#### 14 2.2.2 Observed precipitation extreme events in summer 2020 and event thresholds

15 Considering that the YZR and HHB are located in different latitudes and their peak  
16 precipitations usually occur at different times, we respectively focus on precipitation  
17 extreme events in different months for YZR and HHB.

18 The time evolution of daily summer precipitation over YZR in 2020 and the spatial  
19 distribution of precipitation anomalies in June-July are shown in Figure 2a~b. They  
20 show anomalous heavy precipitation in 2020 occurred in June-July over YZR, and

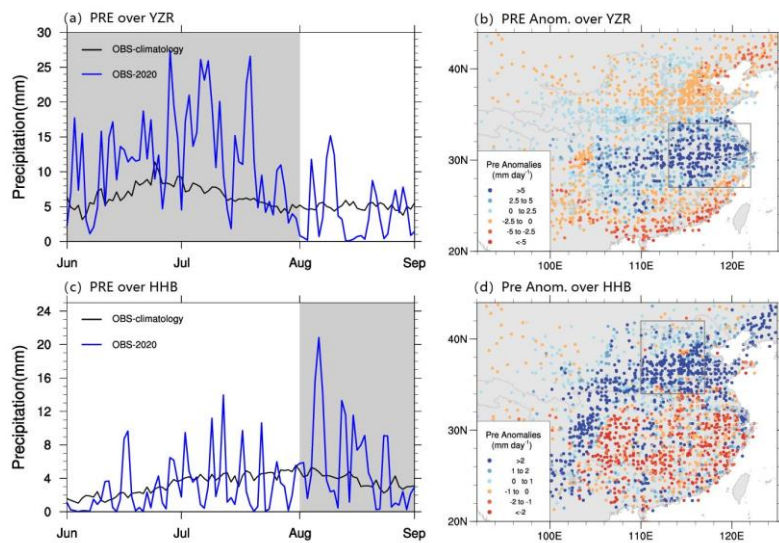
1 therefore the attribution analysis in this study for YZR considers June-July month-scale  
2 precipitation and daily maximum precipitation (RX1day) during these two months.  
3 Details of calculating area averaged monthly precipitation and RX1day in a region are  
4 described in the Supplementary information. The regional averaged precipitation  
5 anomaly relative to the climate mean state in June-July 2020 is 5.2 mm/d and the  
6 regional averaged percentage change of RX1day relative to the climate mean is 40.4%  
7 (Figure 4 a, b), both of which were the highest since 1961. For the YZR region in the  
8 follow-up analysis, 5.2 mm/d and 40.4% were used as the threshold for the monthly  
9 extreme precipitation events and daily extreme precipitation in June-July for the  
10 attribution analysis respectively.

11 Figure 2c~d illustrates the time evolutions of daily summer precipitation in 2020  
12 and the spatial distribution of precipitation anomalies in August. The attribution analysis  
13 will focus on extreme precipitation events in August 2020, which is a period  
14 accompanied by concentrated precipitation. As illustrated in Figure 4c the HHB  
15 regional averaged precipitation anomaly in August 2020 was 1.9 mm/d and the regional  
16 averaged RX1day percentage change was 39.6% above the corresponding climatology  
17 (Figure 4d), both of which were the third highest since 1961. Therefore, the monthly  
18 mean precipitation threshold of 1.9 mm/d and RX1day threshold of 39.6% in August  
19 were used in the attribution analysis for the HHB region. In summary, two precipitation  
20 indices based on observations in summer 2020 over the East China monsoon region  
21 were selected in this study for attribution analysis and future projection. They are  
22 June-July precipitation and RX1day over YZR and monthly precipitation and RX1day  
23 in August over HHB.

24 The atmospheric circulations in 2020 show that the South Asian high (SAH)  
25 extends eastward both in June-July and in August compared to the climatological  
26 position (Figure 3), and the Eastern Asian Subtropical Jet (EASJ) is stronger than  
27 normal, while the western Pacific subtropical high (WPSH) extends westward. The  
28 westward extension of WPSH leads to a large positive geopotential height anomaly and

1 a strong southwest water vapor transport in June-July over YZR. As a result, heavy  
 2 precipitation persists in the YZR region due to the convergence of warm and humid air  
 3 from the south and cold air from the north. This study agrees with the findings of  
 4 numerous studies that show high precipitation in the YZR region when WPSH is strong  
 5 and its ridge extends southward and westward (Jin et al., 2018; Li et al., 2013; Tang et al.  
 6 2021; Nie et al., 2021).

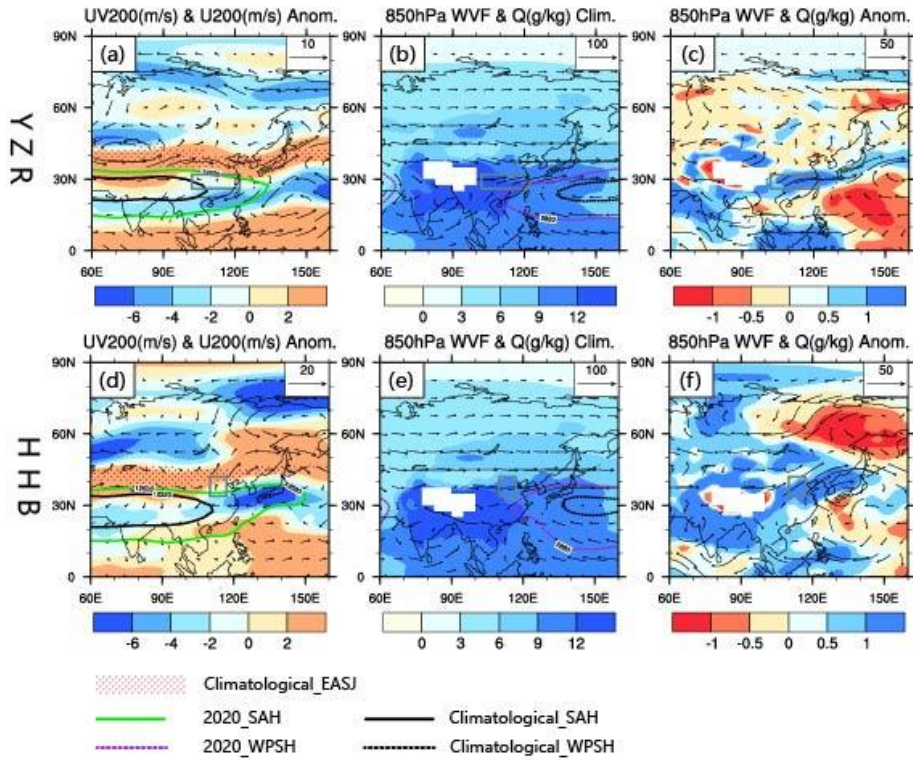
7 Strong southwesterly and southerly winds can be found on the western and  
 8 southern edges of the WPSH in August 2020, transporting water vapor from the Bay of  
 9 Bengal and the western Pacific Ocean to the HHB region. Meanwhile, the northern  
 10 hemisphere polar vortex is dipole-shaped and weaker than normal for the same period,  
 11 and the Westerlies are strong. The high-pressure ridge is near Lake Balkhash. The HHB  
 12 region is controlled by a weak trough over the east of Lake Baikal, so there are more  
 13 weak cold air activities in the HHB region. Cold and warm air convergence causes more  
 14 precipitation in the region than normal. This is consistent with the conclusion that the  
 15 high precipitation in this region is closely related to the weak polar vortex, the  
 16 anomalously strong westerlies in the upper troposphere, and the ridge of subtropical  
 17 high being westward than normal in previous studies (e.g., Zhang et al, 2008; Zhou,  
 18 2009).



19

20 FIGURE 2 (a, c) Time series of observed daily precipitation (mm day<sup>-1</sup>) for summer 2020 (blue) and

1 climatology of 1961-2010 (black) for (a) YZR and (c) HHB. Grey shading indicates June-July and  
 2 August respectively. (b, d) Spatial distributions of observed precipitation anomalies ( $\text{mm day}^{-1}$ ) from  
 3 rain gauges relative to 1961-2010 (b) in June-July over YZR and (d) in August over HHB. Black  
 4 boxes in (b, d) highlight YZR and HHB regions.



5  
 6 FIGURE 3 (a, d) Spatial distributions of 200-hPa wind vector (unit:  $\text{m s}^{-1}$ ) and zonal wind (shaded,  
 7 unit:  $\text{m s}^{-1}$ ) anomalies relative to climatology 1961-2010. (b, c, e, f) Spatial distributions of water  
 8 vapor flux (vector, unit:  $1 \times 10^{-6} \text{ kg hPa}^{-1} \text{ m}^{-1} \text{ s}^{-1}$ ) and specific humidity (shaded, unit:  $\text{g kg}^{-1}$ ) at 850  
 9 hPa for (c, f) summer 2020 anomalies and (b, e) climatology of 1961-2010. The two rows show  
 10 patterns in June-July (top panels) and in August (low panels). The solid green line represents the  
 11 South Asian high (SAH) and the dashed purple line represents the Western Pacific subtropical high  
 12 (WPSH), respectively. The black lines show their summer climatological positions. Red dotted areas  
 13 represent the Eastern Asian Subtropical Jet (EASJ) (zonal wind speeds  $>24 \text{ m s}^{-1}$  at 200hPa).

14

### 15 2.2.3 Attribution methods for extreme events

16 In the historical and historicalNat sets of HadGEM3-GA6 (or ALL and NAT in

1 CMIP6) simulations, the occurrence probability of precipitation events greater than or  
2 equal to the 2020 thresholds were identified as  $P_{ALL}$  and  $P_{NAT}$ , respectively. The risk  
3 ratios (RR) were calculated based on  $RR = P_{ALL} / P_{NAT}$  (National Academies of Sciences  
4 and Medicine, 2016). When  $RR > 1$ , it means that human activities make the event more  
5 likely, and when  $RR < 1$ , it means that human activities make the event less likely. We  
6 estimated the return period of 2020-like extreme events at the end of the 21<sup>st</sup> century by  
7 calculating the probability of precipitation events greater than or equal to the 2020  
8 thresholds for different SSP scenarios which is defined as  $P_{FUT}$ .

9 In the uncertainty analysis, the RR uncertainty with a 90% confidence interval (CI)  
10 was estimated by identifying the empirical 5th and 95th percentile among 1,000 times  
11 resampling model ensemble members by using the Monte Carlo bootstrapping  
12 procedure (Christidis et al. 2013). With each bootstrap, model ensemble simulations are  
13 randomly resampled with replacement to obtain new data of the same length as the  
14 original. For CMIP6 simulations, we calculated the ensemble mean for each model first  
15 and then calculated the multimodel ensemble mean. For probability and RR estimation  
16 for indices, we took all members in the chosen period of selected models as a grand  
17 ensemble.

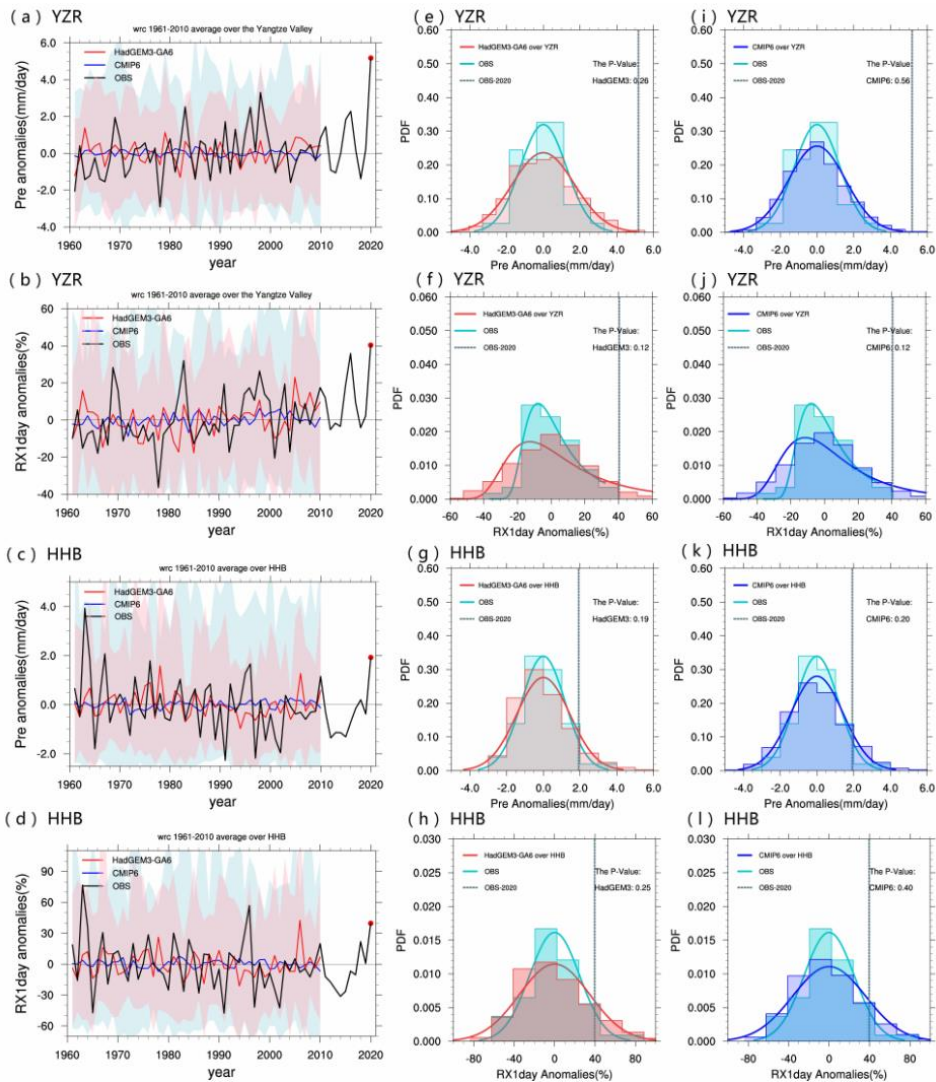
18 In previous studies, it has been shown that the monthly extreme precipitation  
19 anomalies in the East China follow a Gaussian distribution (Alam et al., 2018; Wang et  
20 al., 2019), whereas RX1day in East China is more consistent with the Generalized  
21 Extreme Value (GEV) distribution (Li et al, 2015; Papalexiou and Koutsoyiannis, 2013;  
22 Yang et al., 2013). However, RX1day in northern China follows a normal distribution  
23 (Wang et al., 2017). Therefore, in this study, for the month-scale cumulative  
24 precipitation over two regions, and RX1day over HHB, occurrence probability is  
25 estimated based on the Gaussian distribution and the probability of RX1day over YZR  
26 is based on the GEV distribution.

27

1 **3 RESULTS AND DISCUSSIONS**

2 **3.1 Model evaluation on simulated precipitation and precipitation extremes during**  
 3 **1961-2010**

4 Evaluation of HadGEM3-GA6 and CMIP6 simulations was carried out to  
 5 determine whether these models could accurately reproduce the characteristics of  
 6 precipitation and precipitation extremes in summer over the study regions in East China.  
 7 Time series of observed precipitation anomalies, model simulated precipitation  
 8 anomalies and model uncertainty, and corresponding probability density functions  
 9 (PDFs) for monthly precipitation anomalies and RX1day anomalies are illustrated in  
 10 Figure 4.



11  
 12 **FIGURE 4 (a~d) Time series of anomalous precipitation (a, c, mm/day) and RX1day percentage**



1 anomalies (b, d, %) relative to the climatology of 1961-2010 in June-July over YZR and in August  
2 over HHB for observations and simulated ensemble means of OBS (black solid lines), HadGEM3  
3 model (red solid lines) and CMIP6 multimodel mean (solid blue), and ensemble spreads of  
4 HadGEM3-GA6 (pink shading) and CMIP6 (blue shading), respectively. (e~l) PDFs of anomalous  
5 precipitation and RX1day percentage anomalies in June-July over YZR and in August over HHB  
6 respectively constructed using data from HadGEM3-GA6 historical experiments (red), CMIP6  
7 historical experiments (blue) and OBS (green) from 1961 to 2010. The p-values based on the K-S  
8 test are given in each panel and vertical lines are corresponding values in 2020.

9 Results show that the observational anomalies were encompassed uncertainty  
10 ranges of model simulations (Figure 4 a-d). However, correlation coefficients between  
11 observational and the multi-ensemble mean time series (not shown) are low and these  
12 suggest that the interannual variability of monthly precipitation anomalies and RX1day  
13 anomalies in summer over East China is hard to well simulated considering the  
14 multi-scale feedback processes inherent in the Asian monsoon system. PDFs indicate  
15 that the distributions between HadGEM3-GA6 simulations and OBS precipitation  
16 indices anomalies in summer during 1961–2010 (Figure 4 e-l) cannot be distinguished  
17 at the 0.05 significance level based on the K-S test (with P-value being greater than  
18 0.05), as well as CMIP6 simulations and OBS. The whole 12 CMIP6 models also  
19 passed the test individually (Table S2; Figure S1~S4) and details of model selection are  
20 documented in the Supplementary information. These model evaluations suggest that  
21 both HadGEM3-GA6 and CMIP6 models can be regarded as reliable for attributing  
22 monthly precipitation anomalies and RX1day anomalies in summer 2020 over East  
23 China.

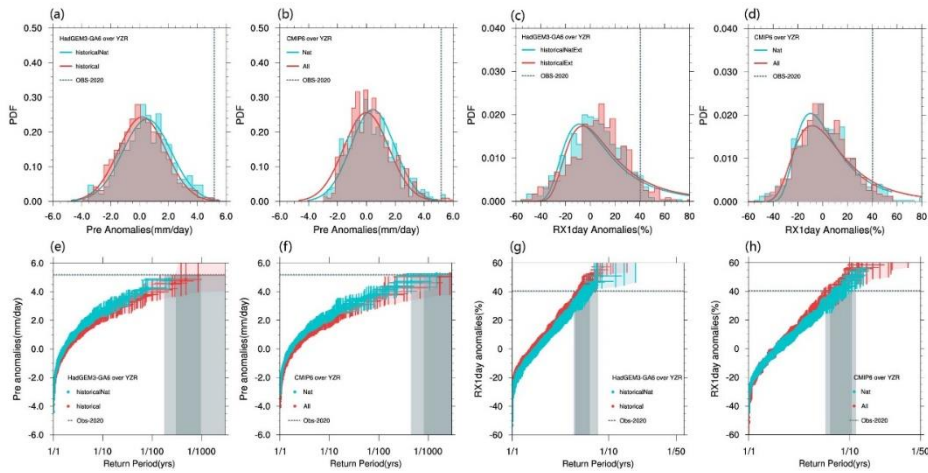
24

## 25 **3.2 Attribution of 2020-like extreme precipitation events in study regions**

### 26 3.2.1 Events in YZR

27 To show the anthropogenic influences on the probability of precipitation extremes  
28 in summer 2020 over YZR, PDFs precipitation anomalies over YZR in June-July 2020

1 and RX1day percentage anomalies and corresponding return periods for these two  
 2 indices in historical (ALL) and historicalNat (NAT) in HadGEM3-GA6 (CMIP6) model  
 3 simulations are illustrated in Figure 5. One of the most important features in PDFs of  
 4 monthly precipitation anomalies is a leftward shift in historical simulations relative to  
 5 historicalNat and this suggests that historical (ALL) simulations tend to have less  
 6 monthly precipitation than historicalNat (NAT) (Figure 5 a, b). HadGEM3-GA6 and  
 7 CMIP6 simulations show consistent risk ratios of 0.41 [90% confidence intervals: 0.30,  
 8 0.47] and 0.53 [90% confidence intervals: 0.21, 1.31], respectively (Figure 6, Table 2).  
 9 These results suggest that anthropogenic forcings significantly reduce the probability of  
 10 the June-July extreme heavy precipitation event similar to 2020 in the YZR region by  
 11 about 59% in HadGEM3 model and 47% in CMIP6 models. As shown in Figure 6, the  
 12 best estimates of RR values in CMIP6 are all less than 1 except NorESM2-LM and  
 13 FGOASLS-g3.

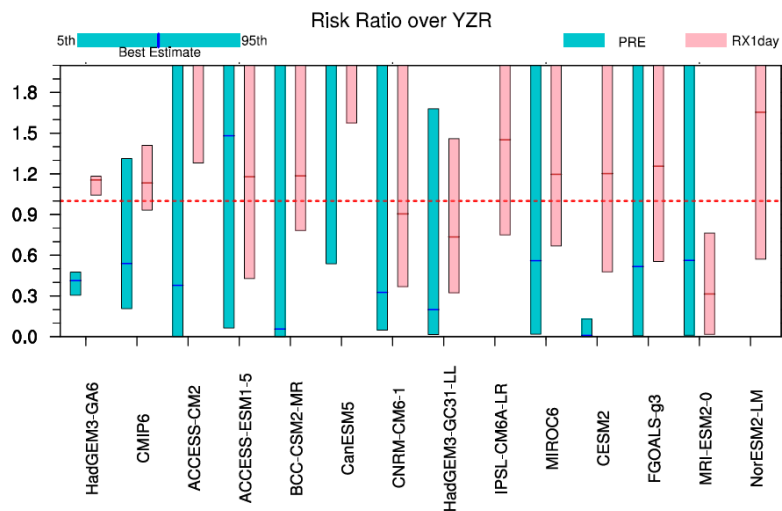


14  
 15 FIGURE 5 PDFs (a-d) and return periods (e-h) for June-July 2020 HadGEM3-GA6 and CMIP6 ALL  
 16 (2011-2020) (red) and NAT (2011-2020) (green) simulated precipitation (a, b, e, f; mm/day) and  
 17 RX1day percentage anomalies (c, d, g, h; %) in the YZR region. Each point in (e-h) represents an  
 18 ensemble member with vertical and horizontal bars being the 5%-95% uncertainty interval of  
 19 precipitation and RX1day percentage anomalies and return periods and grey and dark grey lines  
 20 indicating the uncertainty interval of the return period of the threshold-exceedance in historical and  
 21 historicalNat simulations, respectively. Vertical dotted lines in (a-d) and horizontal dotted lines in

1 (e-f) are corresponding values in 2020.

2 TABLE 2 Return periods and risk ratios of precipitation and RX1day percentage anomalies in  
 3 June-July 2020 over the YZR region simulated by CMIP6 and HadGEM3 models and their  
 4 uncertainty intervals (90% CI)

Index	Models	Return Period (90% CI)	Risk ratios (90% CI)
PRE	HadGEM3-GA6	historical	874.6(300.1, 3363.5)
		historicalNat	361.4(174.6, 969.7)
	CMIP6	ALL	2271.2 (819.2, 9457.3)
		NAT	1223.9 (449.7, 5285.8)
RX1day	HadGEM3-GA6	historical	5.4 (4.4, 6.3)
		historicalNat	6.2 (4.5, 7.7)
	CMIP6	ALL	7.2 (5.7, 10.4)
		NAT	8.4 (6.4, 11.5)



5  
 6 FIGURE 6 Risk ratios and their confidence intervals (90% CI) for the CMIP6 and HadGEM3-GA6  
 7 model simulating precipitation anomalies (green shading) and RX1day percentage anomalies (pink  
 8 shading) in the YZR region. The solid lines indicate the best estimate of precipitation anomalies  
 9 (green lines) and RX1day percentage anomalies (pink lines).

10 Variations in return periods are also indicative (Figure 5e, f) of anthropogenic  
 11 effects reducing the likelihood of 2020-like June-July extreme precipitation events.

1 With only natural forcing, HadGEM3-GA6 shows a return period of 1 in 361 years, and  
2 with ALL forcing, it shows a return period of 1 in 875 years; CMIP6 model simulations  
3 show consistent changes in return period, and it changes from about 1 in 1224 years in  
4 NAT simulations to about 1 in 2271 years in ALL simulations. These attribution results  
5 suggest that human activities have reduced the probability of June-July 2020-like  
6 extreme precipitation events in the YZR region of East China, and this conclusion is  
7 robust for HadGEM3-GA6 and CMIP6 model simulations.

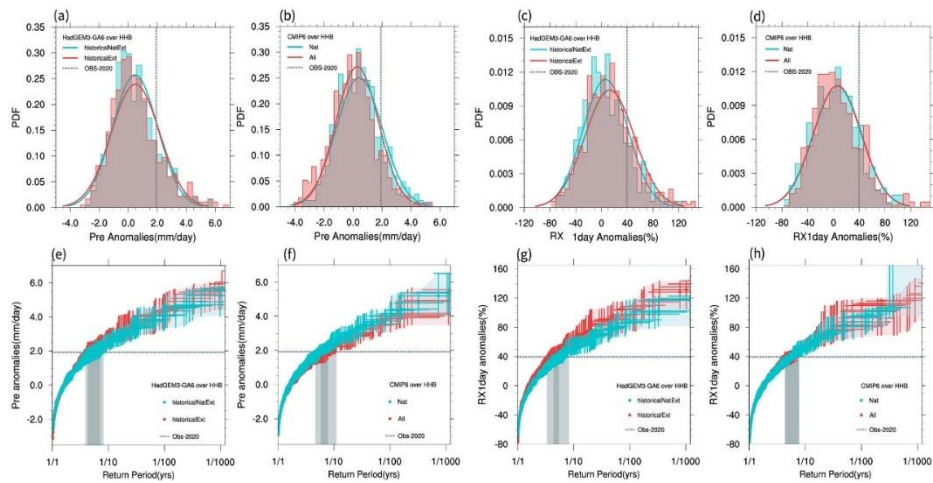
8 In contrast to the monthly precipitation in summer 2020, the analysis of RX1day  
9 shows that the probability of RX1day percentage anomalies larger or similar to  
10 June-July 2020 in historical (ALL) simulations are larger than historicalNat (NAT)  
11 (Figure 5c, d). The risk ratios (RR) estimated by HadGEM3-GA6 and CMIP6 are 1.15  
12 [90% CI: 1.04, 1.18] and 1.13 [90% CI: 0.93, 1.41] (Figure 6, Table 2), implying that  
13 anthropogenic forcings increase the likelihood of summer 2020-like RX1day extreme  
14 heavy precipitation events by about 15% in YZR in HadGEM3-GA6 and 13% in  
15 CMIP6. However, there is some uncertainty in CMIP6 models with most models  
16 showing RR values greater than 1 except for CNRM-CM6-1, HadGEM3-GC3 1-LL,  
17 and MRI-ESM2-0. The variation of the return period (Figure 5g, h) indicates that the  
18 June-July 2020-like RX1day extreme precipitation events are more likely to occur due  
19 to anthropogenic influences. Based on HadGEM3-GA6 simulations, the return period is  
20 about 1 in 6.2 years with only natural forcing and about 1 in 5.4 with ALL forcing.  
21 CMIP6 model simulations show consistent changes in return period, and it changes  
22 from about 1 in 8.4 years in NAT simulations to about 1 in 7.2 years in ALL  
23 simulations.

### 24 25 3.2.2 Events in HHB

26 For 2020-like extreme precipitation events in representative HHB region of East  
27 China, the PDFs of month-scale precipitation and RX1day percentage anomalies in  
28 August show that anthropogenic forcings tend to increase the likelihood of both

1 monthly-scale and RX1day extreme precipitation in HadGEM3-GA6 simulations, with  
 2 the RR of 1.12 [90% CI: 1.11, 1.15] and 1.41 [90% CI: 1.37, 1.48] (Figure 7a, c, Figure  
 3 8, Table 3). The return periods gave consistent conclusions (Figure 7e, g, Table 3), with  
 4 precipitation anomalies and RX1day return periods of 1 in 5.7 and 1 in 5.8 years under  
 5 historicalNat simulations, while they changed to 1 in 5.1 and 1 in 4.1 years under  
 6 historical simulations.

7 CMIP6 simulations show opposite results in monthly-scale extreme precipitation  
 8 but are consistent in RX1day (Figure 7b, d). The PDF distribution curves for ALL  
 9 simulations tend to shift left in comparison with those in NAT simulations, suggesting  
 10 that anthropogenic forcings tend to reduce the likelihood of August-2020-like  
 11 precipitation. Risk ratios (RR) are 0.77 [90% CI: 0.61, 0.94] (Figure 8, Table 3).  
 12 Additionally, the return period demonstrates that the August 2020-like monthly  
 13 precipitation extreme events are less likely to occur due to anthropogenic influences  
 14 (Figure 7f, Table 3). Under the NAT simulation, the return period for monthly  
 15 precipitation anomalies is 5.8 years, but under the ALL simulation is 7.5 years. Except  
 16 for CNRM-CM6-1, CanESM5, and FGOALS-g3, most of CMIP6 models simulate RR  
 17 values of precipitation anomalies that are less than 1 (Figure 8). The RR of RX1day  
 18 estimated by CMIP6 is 1.02 [90% CI: 0.84, 1.27] (Figure 8, Table 3) which is not  
 19 significant since the large spread among different models.



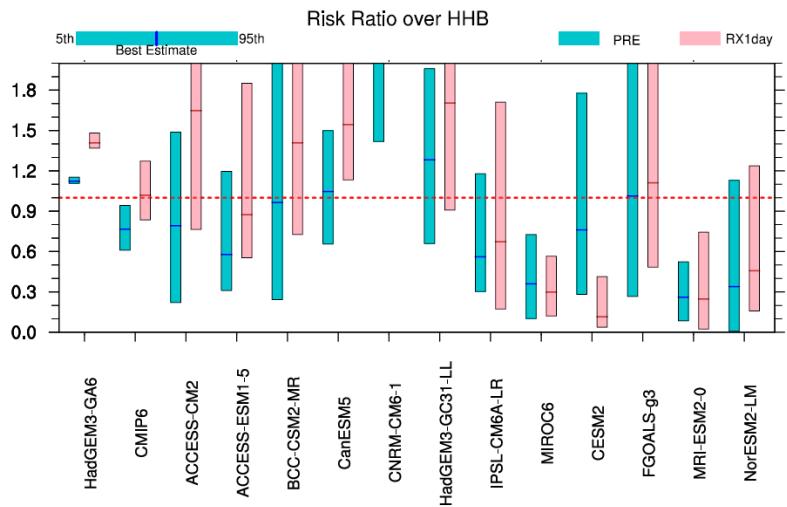
20

21 FIGURE 7 PDFs and return periods for August 2020 HadGEM3-GA6 and CMIP6 ALL (2011-2020)

1 and NAT (2011-2020) simulated precipitation (a, b, e, f; mm/day) and RX1day percentage anomalies  
 2 (c, d, g, h; %) in the HHB region. Each point in (e-h) represents an ensemble member, with vertical  
 3 and horizontal bars being the 5%-95% uncertainty interval of precipitation and RX1day percentage  
 4 anomalies and return periods and grey and dark grey lines indicating the uncertainty interval of  
 5 return period of the threshold-exceedance in historical and historicalNat simulations, respectively.  
 6 Vertical dotted lines in (a-d) and horizontal dotted lines in (e-f) are corresponding values in 2020.

7 TABLE 3 Return periods and risk ratios of precipitation and RX1day percentage anomalies in  
 8 August 2020 in the HHB region simulated by CMIP6 and HadGEM3-GA6 models and their  
 9 uncertainty intervals (90% CI)

Index	Models	Return Period (90% CI)	Risk ratios (90% CI)
PRE	HadGEM3-GA6	historical	5.1 (3.9, 7.1)
		historicalNat	5.7 (4.3, 8.2)
	CMIP6	ALL	7.5 (5.8, 11.1)
		NAT	5.8 (4.7, 7.8)
RX1day	HadGEM3-GA6	historical	4.1 (3.3, 5.4)
		historicalNat	5.8 (4.4, 8.0)
	CMIP6	ALL	5.4 (4.3, 7.7)
		NAT	5.5 (4.4, 7.8)



10  
 11 FIGURE 8 Risk ratios and their uncertainty intervals (90% CI) for the CMIP6 and HadGEM3

1 models simulating precipitation anomalies (green shading) and RX1day percentage anomalies (pink  
2 shading) in the HHB region. The solid lines indicate the best estimate of precipitation anomalies  
3 (green lines) and RX1day percentage anomalies (pink lines).

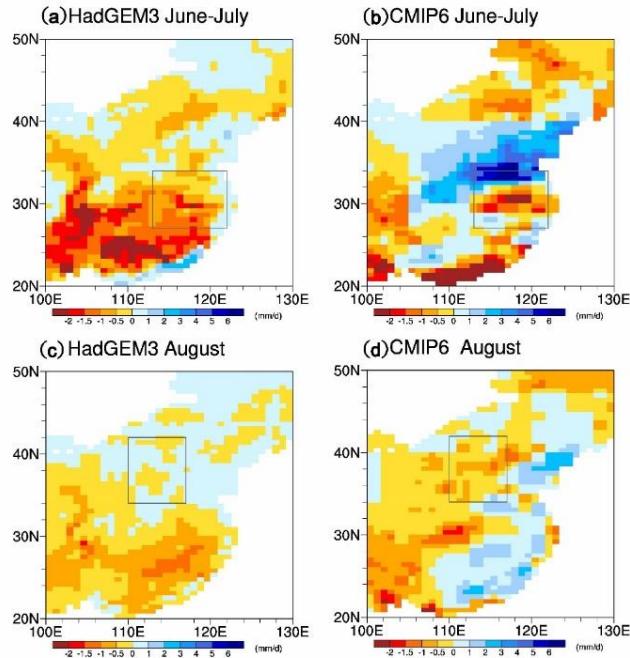
### 4 5 3.2.3 Difference between the two attribution systems

6 The main attribution results based on two attribution systems in two regions of  
7 East China are summarized in Table 4. These results show consistent conclusions for  
8 June-July precipitation extremes and RX1day in 2020 over the YZR region between  
9 CMIP6 and HadGEM3-GA6 model simulations. However, attribution results are  
10 inconsistent in the HHB region between the two models, especially for August monthly  
11 precipitation in 2020. HadGEM3-GA6 simulations show an increase of likelihood by  
12 12% while CMIP6 models show a decrease of 23% based on anthropogenic forcing.  
13 The reasons responsible for these contrasting results between two different systems  
14 need to be investigated further. These contrasting attribution results suggest that one has  
15 to draw the attribution conclusion carefully and multiple methods might need to make  
16 helpful attribution conclusions in this region.

17 Spatial patterns of multimodel mean (ensemble mean for HadGEM3-GA6)  
18 changes in June-July and August precipitation in response to anthropogenic forcings  
19 among two systems over East China are illustrated in Figure 9. In June-July, two models  
20 show common features of reduced precipitation in YZR, which is consistent with  
21 reduced likelihood of extreme monthly precipitation in this region. However, there are  
22 some different spatial distributions of precipitation anomalies. The main feature in  
23 CMIP6 models is a dipole pattern of precipitation anomalies with reduced precipitation  
24 over YZR and increased precipitation HHB. In contrast, HadGEM3-GA6 shows  
25 reduced precipitation in both regions.

26 In August, CMIP6 models show a dipole pattern with reduced precipitation over  
27 the HHB region and increased precipitation to the south while HadGEM3-GA6 shows  
28 an opposite dipole with increased precipitation in HHB and reduced precipitation over

1 large parts of southern China. These different spatial distributions of multimodel mean  
 2 monthly precipitation over East China in response to anthropogenic forcing can explain  
 3 different attribution results in the HHB region between two models.



4  
 5 FIGURE 9 Spatial distributions of precipitation difference ( $\text{mm day}^{-1}$ ) between with and without  
 6 anthropogenic forcing by using HadGEM3 (a, d) and CMIP6 (b, d) models in June-July (a, b) and in  
 7 August (c, d). Black boxes in (a, b) and (c-d) highlight YZR and HHB regions.

8 TABLE 4 The human influence on Pre and Rx1day for YZR and HHB

		YZR Month-scale Pre	YZR Rx1day	HHB Month-scale Pre	HHB Rx1day
Human influence	CMIP6	Decrease	Increase	Decrease	Increase
	HadGEM3	Decrease	Increase	Increase	Increase
Risk Ratio	CMIP6	0.53 (0.21,1.31)	1.13 (0.93, 1.41)	0.77 (0.61, 0.94)	1.02 (0.84, 1.27)
	HadGEM3	0.41 (0.30,0.47)	1.15 (1.04, 1.18)	1.12 (1.11,1.15)	1.41 (1.37, 1.48)

9 CMIP6 models are fully coupled models and HadGEM3-GA6 is an atmospheric  
 10 only model. Why two models show some different features in seasonal evolutions of  
 11 precipitation in response to anthropogenic forcing? This is an important question.  
 12 Previous studies showed that anthropogenic forcings affect regional precipitation



1 through both thermodynamical contributions related to change in humidity in the  
2 atmosphere and dynamical contributions related to changes in atmospheric circulation  
3 (e.g., Tian et al 2018, Guo et al. 2023, Li et al. 2022). Thermodynamical contributions  
4 showed less spatial variations while dynamical contributions show large spatial  
5 variations related to changes in atmospheric circulation (e.g., Tian et al. 2018, Guo et al.  
6 2023, Li et al. 2022). It would be valuable to investigate atmospheric circulation and  
7 thermal variable response to anthropogenic forcing in CMIP6 models and  
8 HadGEM3-GA6 model to understand regional precipitation changes. However, to  
9 address this is beyond the scope of this study.

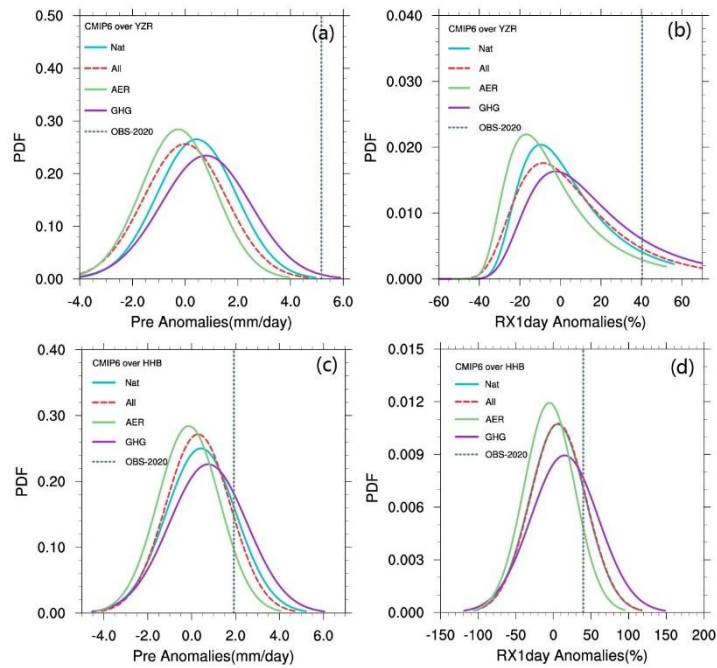
#### 11 3.2.4 Contributions from different forcing factors of human activities

12 Based on the attribution analysis above, it is suggested that anthropogenic forcings  
13 have contributed to the occurrence of extreme precipitation events similar to those in the  
14 summer 2020 in two regions over East China. As the two most important anthropogenic  
15 forcing factors, what are the respective contributions of GHG and AER to the changes  
16 in the likelihood of precipitation events? To answer this question, the DAMIP  
17 simulations of the historical, historicalNat, historicalAER, and historicalGHG  
18 experiments were used to quantify the contributions of GHG and AER on the likelihood  
19 of June-July and August precipitation and RX1day percentage anomalies in summer  
20 2020 in the YZR and HHB regions.

21 PDFs and return periods due to different forcings are shown in Figure 10 and Table  
22 5. Results indicate that anthropogenic aerosol emissions have reduced the likelihood of  
23 2020-like month-scale precipitation and corresponding RX1day extreme events in  
24 June-July over YZR and August over HHB. These changes correspond to increases in  
25 return period for YZR and HHB precipitation events and RX1day in both regions. The  
26 greenhouse gas emissions from human activities increase the likelihood of both events,  
27 leading to decreases of return period for summer 2020-like events. As the influences of  
28 aerosol emissions are stronger than those of changes in GHG, human activities have

1 reduced the likelihood of the monthly extreme precipitation over both YZR and HHB.  
 2 TABLE 5 Return periods and their uncertainty intervals (90% CI) for precipitation and RX1day  
 3 percentage anomalies in June-July over YZR and in August over HHB simulated by CMIP6 under  
 4 different forcing factors.

Region	Models	PRE Return Period (90% CI)	RX1day Return Period (90% CI)
YZR	CMIP6	ALL	2271.2 (819.2, 9457.3)
		NAT	1223.9 (449.7, 5285.8)
		AER	18682.9 (4487.1, 174762.7)
		GHG	201.0 (101.6, 606.9)
HHB	CMIP6	ALL	7.5 (5.8, 11.1)
		NAT	5.8 (4.7, 7.8)
		AER	14.1 (8.7, 27.3)
		GHG	3.9 (3.2, 5.2)



5  
 6 FIGURE 10 PDFs of CMIP6 simulated 2020-like extreme precipitation and RX1day events for (a, c)  
 7 YZR regions in June-July and (b, d) HHB in August and under different factors of human forcing.  
 8 Vertical dotted lines are corresponding values in 2020.

1 The above conclusion is consistent with the results by Tian (2018) that increasing  
2 GHG leads to increased precipitation by increasing the moisture transport convergence  
3 over eastern China, while aerosol forcing leads to divergent wind anomalies over  
4 northern China and reduced precipitation by weakening the EASM. In contrast, GHG  
5 induced increase of the probability of RX1day similar to the 2020 events in both regions  
6 is larger than AER induced decrease, leading to an increase of the probability of  
7 RX1day similar to the 2020 events although the increased probability is not significant  
8 due to large spread among different models in the HHB region.

### 9 10 **3.3 Projected changes in the likelihood of similar extreme precipitation events in** 11 **summer 2020 at the end of the 21st century**

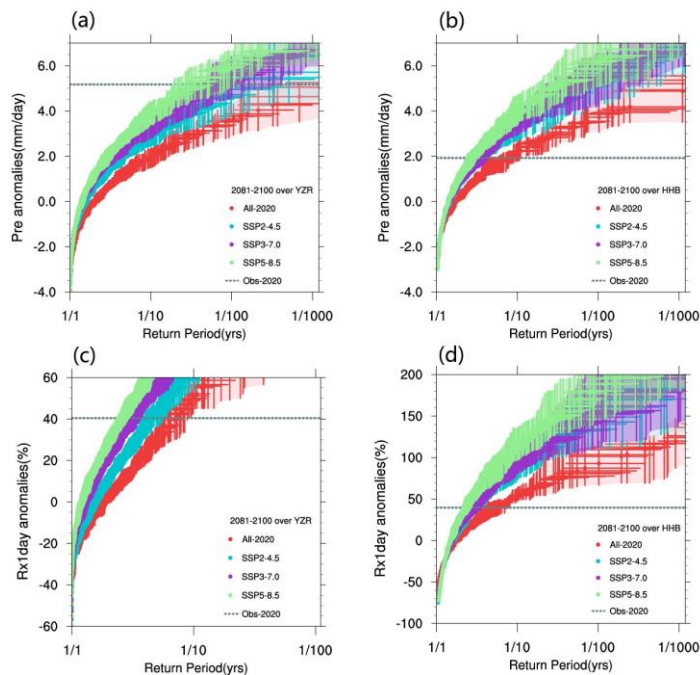
12 As greenhouse gas emissions will increase and anthropogenic aerosol emissions  
13 will decrease at the end of the 21<sup>st</sup> century, how will the probability of 2020-like  
14 extreme precipitation events happening over China by changing with global warming?  
15 To address this question, the CMIP6 simulations under scenarios SSP2-4.5, SSP3-7.0,  
16 and SSP5-8.5 were analyzed, and results on return periods are shown in Figure 11 and  
17 Table 6. One of the most important features is the decrease of return periods for monthly  
18 precipitation anomalies and RX1day percentage anomalies, although the magnitude of  
19 decrease depends on the scenarios. The largest change is anticipated for heavy  
20 precipitation over YZR in June–July 2020. and the return period for this kind of  
21 extremely rare event changes from 1 in 2271.2 years in present-day climate to 1 in  
22 202.8/76.2/36.4 yearly events at the end of the 21<sup>st</sup> century under different scenarios.  
23 The above indicates an increase of the likelihood of this kind of event by more than 10  
24 times.

25 The return period of 2020-like RX1day extreme precipitation events similar to that  
26 occurred over YZR changes from 1 in 7.2 years to 1 in 4.6/3.2/2.6 yearly events,  
27 suggesting this kind of event would be about doubled at the end of the 21<sup>st</sup> century.  
28 Under all three scenarios, return periods of heavy precipitation events that occurred in

1 August 2020 over the HHB region are shortened from 1 in 7.5 years in present day  
 2 climate to 1 in 3.4/3.2/2.8 years at the end of the 21<sup>st</sup> century, and RX1day is shortened  
 3 from 1 in 5.4 years to 1 in 2.9/2.8/2.3 years, suggesting that August 2020-like heavy  
 4 precipitation events over the HHB region would become more frequent.

5 TABLE 6 Return periods and their confidence interval (90% CI) for 2020-like extreme precipitation  
 6 and RX1day percentage anomalies in June-July over YZR and August over HHB simulated by  
 7 CMIP6 for different future scenarios at the end of the 21st century.

Region	Models	PRE Return Period (90% CI)	RX1day Return Period (90% CI)
YZR	CMIP6	ALL-2020	2271.2 (819.2, 9457.3)
		SSP2-4.5	202.8 (99.6, 532.4)
		SSP3-7.0	76.2 (41.6, 185.5)
		SSP5-8.5	36.4 (24.9, 74.2)
HHB	CMIP6	ALL-2020	7.5 (5.8, 11.1)
		SSP2-4.5	3.4 (2.9, 4.4)
		SSP3-7.0	3.2 (2.8, 4.1)
		SSP5-8.5	2.8 (2.4, 3.4)



8  
 9 FIGURE 11 Return period and its uncertainty interval for 2020-like extreme precipitation anomalies

1 (a, b) and RX1day percentage anomalies (c, d) and their comparisons. (a, c) for June-July in the YZR  
2 region, (b, d) for August in the HHB region. Each point in (a-d) represents an ensemble member with  
3 vertical and horizontal bars being the 5%-95% uncertainty interval of precipitation and RX1day  
4 percentage anomalies and return periods. Horizontal dotted lines in (a-d) are corresponding values in  
5 2020.

#### 6 7 **4 CONCLUSIONS**

8 Historical simulation experiments using HadGEM3-GA6 and CMIP6 models with  
9 and without anthropogenic influence were conducted to attribute extremely heavy  
10 precipitation events in summer of 2020 over East China. We focus on a comparative  
11 study of the attribution results of monthly extreme precipitation and daily extreme  
12 precipitation in the mid-lower reaches of the Yangtze River basin as the representative  
13 south region and the lower reaches of the Yellow River- Hai River basin as the  
14 representative north region of the East China monsoon region. The main conclusions are  
15 as follows.

16 (1) For month-scale extreme precipitation events in the south of the East China  
17 monsoon region, human activities have reduced the likelihood of occurrence of this kind  
18 event. In other words, the occurrence of such extreme precipitation events is largely  
19 dependent on natural variability. For RX1day extreme precipitation events,  
20 anthropogenic factors have increased their probability both in north and south of the  
21 East China monsoon region. However, attribution results for August monthly  
22 precipitation in 2020 are inconsistent in the HHB region between two models, related to  
23 different spatial distributions of CMIP6 multi-model mean (HadGEM3-GA6  
24 multi-ensemble mean) monthly precipitation over East China in response to  
25 anthropogenic forcing.

26 Our result is consistent with those of previous studies that human influence may  
27 have a dramatic impact on extreme precipitations (Min et al., 2011; Kirchmeier-Young  
28 et al., 2020; Paik et al., 2020). While Natural variability will dominate interannual

1 variations in seasonal extreme precipitation in regional scales over the climate change  
2 signal (Martel et al., 2018; Li et al., 2021a). For 2020 extreme precipitation,  
3 anthropogenic forcing has decreased the likelihood of the month-scale extreme rainfall  
4 that was observed in the lower Yangtze River in 2020 (Zhou et al., 2021; Lu et al., 2022;  
5 Ma et al., 2022; Tang et al., 2022).

6 (2) In terms of different factors of human activities, anthropogenic aerosol forcing  
7 reduces both 2020-like monthly extreme precipitation and RX1day events; greenhouse  
8 gases increase the likelihood of both. As the influences of anthropogenic aerosol  
9 emissions are stronger than those of changes in GHG on monthly precipitation, human  
10 activities have reduced the likelihood of the monthly extreme precipitation over both  
11 YZR and HHB in CMIP6 model simulations. In contrast, GHG induced increase of the  
12 probability of RX1day similar to the 2020 events in both regions is larger than AER  
13 induced decrease, leading to an increase of the probability of RX1day similar to the  
14 2020 events.

15 Our findings support the widely held belief that increased aerosol forcing reduces  
16 the severity of precipitation in China's eastern monsoon region (Zhao et al., 2006;  
17 Zhang et al., 2020). This is also consistent with a recent study by Yang et al. (2022) who  
18 found that the reduction of aerosol emissions during the COVID-19 pandemic led to  
19 abnormal land warming in eastern China, which enhanced the atmospheric circulation  
20 between eastern China, the South China Sea and the Philippine Sea, causing water  
21 vapor to be transported to China, ultimately leading to increased precipitation in Eastern  
22 China.

23 (3) Both the monthly extreme precipitation and RX1day events will become more  
24 frequent and the recurrence periods will shorten in both study regions by the end of the  
25 21<sup>st</sup> century. High emission scenarios show a greater increase in likelihood and a  
26 decrease in return period, which indicates that extreme precipitation risk increases with  
27 the concentration of greenhouse gases. Given the devastating impacts of these  
28 precipitation extreme events, our results suggest people will encounter much fiercer

1 changes of precipitation and precipitation extreme over China in the future and China  
2 would face a challenge to take adaptation measures to cope with those projected  
3 changes. Urgent actions need to be taken to control greenhouse gases emissions to avoid  
4 worse-case scenarios and to limit the damages from the increased risk of extreme heavy  
5 precipitation events. Carbon peaking and carbon neutrality should be realized as early as  
6 possible by policymakers through implementing sustainable development strategies and  
7 optimizing the energy structure.

## 8 **AUTHOR CONTRIBUTIONS**

10 Rouke Li: Conceptualization; methodology; investigation; visualization; writing –  
11 original draft; writing – review and editing. Xiaodong Liu: Conceptualization; writing –  
12 review and editing; funding acquisition. Ying Xu: Software, writing – review & editing,  
13 funding acquisition. Buwen Dong: Supervision; methodology; writing – review and  
14 editing.

## 16 **ACKNOWLEDGEMENTS**

17 We thank two anonymous reviewers and editor for their constructive comments and  
18 suggestions, which strengthened the manuscript considerably. This work is supported by  
19 the National Natural Science Foundation of China (41991254) and China Three Gorges  
20 Corporation (0704081), and the key Youth Innovation Team of China Meteorological  
21 Administration (CMA2023QN15). We thank the team of model developers and  
22 infrastructure experts for conducting the large HadGEM3-GA6 simulation campaign,  
23 and the Climate Science for Service Partnership (CSSP)-China programme for  
24 providing data access. We acknowledge the World Climate Research Programme’s  
25 Working Group on Coupled Modelling and the individual modelling groups for their  
26 roles in making CMIP6 data available.

1 ORCID

2 Rouke Li. <https://orcid.org/0000-0002-9774-9370>

3 Xiaodong Liu. <https://orcid.org/0000-0003-0355-5610>

4 Buwen Dong. <https://orcid.org/0000-0003-0809-7911>

5

## 6 REFERENCES

- 7 Alam, M.A., Farnham, C. & Emura, K. (2018) Best-fit probability models for maximum monthly rainfall  
8 in bangladesh using gaussian mixture. *Geosciences*, **8**(4), 138. Available from:  
9 <https://doi.org/10.3390/geosciences8040138>
- 10 Bellouin, N., Quaas, J., Gryspeerdt, E., Kinne, S., Stier, P., Watson-Parris, D. et al. (2020). Bounding  
11 global aerosol radiative forcing of climate change. *Reviews of Geophysics*, **58**, e2019RG000660.  
12 Available from: <https://doi.org/10.1029/2019RG000660>
- 13 Boucher, O., Randall, D., Artaxo, P., Bretherton, C., Feingold, G., Forster, P. et al. (2013) *Clouds and*  
14 *aerosols. In Climate Change 2013: The Physical Science Basis. Contribution of Working Group I to*  
15 *the Fifth Assessment Report of the Intergovernmental Panel on Climate Change*. Cambridge  
16 University Press, DOI:10.1017/CBO9781107415324.016
- 17 China Ministry of Emergency Management. (2021). *National Natural Disaster Fundamentals 2020*,  
18 accessed 08 January 2021, Available from:  
19 [https://www.mem.gov.cn/xw/yjglbgzdt/202101/t20210108\\_376745.shtml](https://www.mem.gov.cn/xw/yjglbgzdt/202101/t20210108_376745.shtml)
- 20 China Meteorological Administration. (2021). *China Climate Bulletin 2020*, Beijing: China  
21 Meteorological Press.
- 22 China Meteorological Administration (2022) *Blue Book on Climate Change in China 2021*, Beijing:  
23 Science Press.
- 24 Chen, G., Wang, W.C. & Chen, J.P. (2018) Circulatory responses to regional aerosol climate forcing in  
25 summer over East Asia. *Climate Dynamics*, **51**(11), 3973-3984. Available from:  
26 <https://doi.org/10.1002/joc.6887>
- 27 Chen, H.P. & Sun, J.Q. (2017) Contribution of human influence to increased daily precipitation extremes  
28 over China. *Geophysical Research Letters*, **44**, 2436-2444. Available from:



1 <https://doi.org/10.1002/2016GL072439>

2 Christidis, N., Stott, P.A., Scaife, A.A., Arribas, A., Jones, G.S., Copsey, D. et al. (2013) A New  
3 HadGEM3-A-Based System for Attribution of Weather- and Climate-Related Extreme Events.  
4 *Journal of Climate*, **26**, 2756-2783. Available from: <https://doi.org/10.1175/JCLI-D-12-00169.1>.

5 Ciavarella, A., Christidis, N., Andrews, M., Groenendijk, M., Rostron, J., Elkington, M. et al. (2018)  
6 Upgrade of the HadGEM3-A based attribution system to high resolution and a new validation  
7 framework for probabilistic event. *Weather and Climate Extremes*, **20**, 9-32. Available from:  
8 <https://doi.org/10.1016/j.wace.2018.03.003>.

9 Cressman, G. P. (1959) An Operational Objective Analysis System. *Monthly Weather Review*, **87**,  
10 367–374. Available from: [https://doi.org/10.1175/1520-0493\(1959\)087<0367:AOOAS>2.0.CO;2](https://doi.org/10.1175/1520-0493(1959)087<0367:AOOAS>2.0.CO;2)

11 Diao, C., Xu, Y. & Xie, S.P. (2021) Anthropogenic aerosol effects on tropospheric circulation and sea  
12 surface temperature (1980-2020): Separating the role of zonally asymmetric forcings. *Atmosphere*  
13 *Chemical and Physics*, **21**(24), 18499-18518. Available from:  
14 <https://doi.org/10.5194/acp-21-18499-2021>

15 Dong, S.Y., Sun, Y. & Li, C. (2020) Detection of human influence on precipitation extremes in Asia.  
16 *Journal of Climate*, **33**, 5293–5304. Available from: <https://doi.org/10.1175/JCLI-D-19-0371.1>.

17 Dong, S.Y., Sun, Y., Li, C., Zhang, X.B., Min, S. & Kim, Y. (2021) Attribution of extreme precipitation  
18 with updated observations and CMIP6 simulations. *Journal of Climate*, **34**(3), 871–881. Available  
19 from: <https://doi.org/10.1175/jcli-d-19-1017.1>

20 Eyring, V., Bony, S., Meehl, G. A., Senior, C. A., Stevens, B., Stouffer, R. J. et al. (2016) Overview of the  
21 coupled model intercomparison project phase 6 (CMIP6) experimental design and organization.  
22 *Geoscientific Model Development*, **9**, 1937–1958. Available from:  
23 <https://doi.org/10.5194/gmd-9-1937-2016>

24 Gillett, N. P., Shiogama, H., Funke, B., Hegerl, G., Knutti, R., Matthes, K. et al. (2016) The Detection and  
25 Attribution Model Intercomparison Project (DAMIP v1.0) contribution to CMIP6. *Geoscientific*  
26 *Model Development*, **9**, 3685-3697. Available from: <https://doi.org/10.5194/gmd-9-3685-2016>

27 Guo, Y., Dong, B.W. & Zhu, J.S. (2023) Anthropogenic impacts on changes in summer extreme  
28 precipitation over China during 1961–2014: roles of greenhouse gases and anthropogenic aerosols.

1 *Climate Dynamic*, **60**, 2633–2643. Available from: <https://doi.org/10.1007/s00382-022-06453-4>

2 He, J. & Soden, B.J. (2015) Anthropogenic Weakening of the Tropical Circulation: The Relative Roles of  
3 Direct CO<sub>2</sub> Forcing and Sea Surface Temperature. *Journal of Climate*, **28**(22), 8728-8742. Available  
4 from: <https://doi.org/https://doi.org/10.1175/JCLI-D-15-0205.1>

5 IPCC. (2021) *Climate Change 2021: The Physical Science Basis. Contribution of Working Group I to the*  
6 *Sixth Assessment Report of the Intergovernmental Panel on Climate Change of the United States of*  
7 *America*. Cambridge University Press, Cambridge, United Kingdom and New York, NY, USA.  
8 DOI:10.1017/9781009157896.

9 Ji, P., Yuan, X., Jiao, Y., Wang, C., Han, S. & Shi, C. (2020) Anthropogenic Contributions to the 2018  
10 Extreme Flooding over the Upper Yellow River Basin in China. *Bulletin of the American*  
11 *Meteorological Society*, **101**(1), S89-S94. Available from:  
12 <https://doi.org/10.1175/BAMS-D-19-0105.1>

13 Jin, A.H., Zeng, G., YU, Y., Deng, W.T. & Li, Z.X. (2018) Influence of the meridional and latitudinal  
14 position configuration of South Asian high pressure and western Pacific subtropical high on summer  
15 precipitation in eastern China (in Chinese). *Journal of Tropical Meteorology*, **34**(6), 806-818.  
16 Available from: <https://doi.org/10.16032/j.issn.1004-4965.2018.06.009>

17 Kalnay, E., Kanamitsu, M., Kistler, R., Collins, W., Deaven, D., Gandin, L. et al. (1996) The  
18 NCEP/NCAR 40-Year Reanalysis Project. *Bulletin of the American Meteorological Society*, **77**(3),  
19 437-472. Available from: [https://doi.org/10.1175/1520-0477\(1996\)077<0437:TNYRP>2.0.CO;2](https://doi.org/10.1175/1520-0477(1996)077<0437:TNYRP>2.0.CO;2)

20 Kharin, V.V., Zwiers, F.W., Zhang, X.B. & Wehner, M.F. (2013) Changes in Temperature and  
21 Precipitation Extremes in the CMIP5 Ensemble. *Climatic Change*. **119**, 345-357. Available from:  
22 <https://doi.org/10.1007/s10584-013-0705-8>.

23 Kirchmeier-Young, M.C. & Zhang, X. (2020) Human influence has intensified extreme precipitation in  
24 North America. *Proceedings of the National Academy of Sciences*, **117**, 13308-13313. Available  
25 from: <https://doi.org/10.1073/pnas.1921628117>

26 Li, C., Tian, Q., Yu, R., Zhou, B., Xia, J., Burke, C. et al. (2018) Attribution of extreme precipitation in  
27 the lower reaches of Yangtze River during May 2016. *Environmental Research Letters*. **13**(1),  
28 014015. Available from: <https://doi.org/10.1088/1748-9326/aa9691>.

- 1 Li, H., Zhou, S.W. & Wang, Y.F. (2013) A review on the relationship between subtropical high anomalies  
2 over West Pacific and summer precipitation in the middle-lower reaches of the Yangtze River(in  
3 Chinese). *Journal of Meteorology and Environment*, **29**(1), 93-102. Available from:  
4 <https://doi.org/10.3969/j.issn.1673-503X.2013.01.016>
- 5 Li, R.K., Li, D.L., Nanding, N., Wang, X., Fan, X.W., Chen, Y. et al. (2021a) Anthropogenic influences  
6 on heavy precipitation during the 2019 extremely wet rainy season in Southern China. *Bulletin of the*  
7 *American Meteorological Society*. **102**(1), S103-S109. Available from:  
8 <https://doi.org/10.1175/BAMS-D-20-0135.1>.
- 9 Li, T., Wang, Y., Wang, B., Ting, M., Ding, Y., Sun, Y. et al. (2022) Distinctive South and East Asian  
10 Monsoon circulation responses to global warming. *Science Bulletin*, **67**(7), 762-770. Available from:  
11 <https://doi.org/10.1016/j.scib.2021.12.001>.
- 12 Li, W., Chen, Y. & Chen, W. (2021b) The emergence of anthropogenic signals in mean and extreme  
13 precipitation trends over China by using two large ensembles. *Environmental Research Letters*, **16**(1),  
14 014052. Available from: <https://doi.org/10.1088/1748-9326/abd26d>
- 15 Li, Z., Li, Z., Zhao, W. & Wang, Y. (2015) Probability Modeling of Precipitation Extremes over Two  
16 River Basins in Northwest of China. *Advances in Meteorology*, **2015**(6), 1-13. Available from:  
17 <https://doi.org/10.1155/2015/374127>
- 18 Lin, L., Gettelman, A., Fu, Q. & Xu, Y. (2018) simulated differences in 21<sup>st</sup>-century aridity due to  
19 different scenarios of greenhouse gases and aerosols. *Climatic Change*, **146**(3), 407-422. Available  
20 from: <https://doi.org/10.1007/s10584-016-1615-3>
- 21 Lu, C., Chen, R., Jiang, J. & Ullah, S. (2020) Anthropogenic influence on 2019 persistent drought in  
22 southwestern China. *Bulletin of the American Meteorological Society*, **101**(1), S65-S70. Available  
23 from: <https://doi.org/10.1175/BAMS-D-20-0128.1>
- 24 Lu, C., Sun, Y. & Zhang, X. (2022) The 2020 Record-Breaking Mei-yu in the Yangtze River Valley of  
25 China: The Role of Anthropogenic Forcing and Atmospheric Circulation. *Bulletin of the American*  
26 *Meteorological Society*, **103**, S98-S104. Available from:  
27 <https://doi.org/10.1175/BAMS-D-21-0161.1>.
- 28 Ma, Y., Z. Hu, X. Meng, F. Liu & W. Dong (2022) Was the Record-Breaking Mei-yu of 2020 Enhanced

1 by Regional Climate Change? *Bulletin of the American Meteorological Society*, **103**, S76–S82.  
2 Available from: <https://doi.org/10.1175/BAMS-D-21-0187.1>.

3 Martel, J.L., Mailhot, A., Brissette, F. & Caya, D. (2018) Role of Natural Climate Variability in the  
4 Detection of Anthropogenic Climate Change Signal for Mean and Extreme Precipitation at Local and  
5 Regional Scales. *Journal of Climate*, **31**(11), 4241-4263. Available from:  
6 <https://doi.org/10.1175/JCLI-D-17-0282.1>

7 Min, S.K., Zhang, X., Zwiers, F.W. & Hegerl, G.C. (2011) Human contribution to more-intense  
8 precipitation extremes. *Nature*, **470**(7334), 378-381. Available from:  
9 <https://doi.org/10.1038/nature09763>

10 Myhre, G., Shindell, D., Breon, F., Collins, W., Fuglestedt, J., Huang, J. et al. (2014) *Anthropogenic and*  
11 *Natural Radiative Forcing. In: Climate Change 2013: The Physical Science Basis. Contribution of*  
12 *Working Group I to the Fifth Assessment Report of the Intergovernmental Panel on Climate Change.*  
13 Cambridge University Press, Cambridge, United Kingdom and New York, NY, USA.

14 Nanding, N., Chen, Y., Wu, H., Dong, B.W., Tian, F.X., Lott, F. et al. (2020) Anthropogenic influences on  
15 2019 July precipitation extremes over the mid–lower reaches of the Yangtze River. *Frontiers in*  
16 *Environmental Science*, **8**, 603601. Available from: <https://doi.org/10.3389/fenvs.2020.603061>

17 National Academies of Sciences, Engineering and Medicine. (2016) *Attribution of Extreme Weather*  
18 *Events in the Context of Climate Change.* Washington, DC: The National Academies Press.

19 Nie, J., Liu, P. & Zhao, C. (2021) Research on Relationship between Various Indexes of the Western  
20 North Pacific Subtropical High and Summer Precipitation in Eastern China (in Chinese).  
21 *Atmospheric Science*, **45**(4), 833-850. Available from:  
22 <https://doi.org/10.3878/j.issn.1006-9895.2009.20160>

23 O’Gorman, P. (2012) Sensitivity of tropical precipitation extremes to climate change. *Nature Geoscience*,  
24 **5**(10), 697-700. Available from: <https://doi.org/10.1038/ngeo1568>

25 O’Neill, B.C., Tebaldi, C., van Vuuren, D.P., Eyring, V., Friedlingstein, P., Hurtt, G. et al. (2016) The  
26 Scenario Model Intercomparison Project (ScenarioMIP) for CMIP6. *Geoscientific Model*  
27 *Development*, **9**(9), 3461-3482. Available from: <https://doi.org/10.5194/gmd-9-3461-2016>

28 Paik, S., Min, S.-K., Zhang, X., Donat, M. G., King, A. D. & Sun, Q. (2020). Determining the

1 anthropogenic greenhouse gas contribution to the observed intensification of extreme precipitation.  
2 *Geophysical Research Letters*, **46**, e2019GL086875. Available from:  
3 <https://doi.org/10.1029/2019GL086875>

4 Papalexiou, S.M. & Koutsoyiannis, D. (2013) Battle of extreme value distributions: a global survey on  
5 extreme daily rainfall. *Water Resources Research*, **49**(1), 187-201. Available from:  
6 <https://doi.org/10.1029/2012WR012557>

7 Papalexiou, S.M. & Montanari, A. (2019) Global and Regional Increase of Precipitation Extremes Under  
8 Global Warming. *Water Resources Research*, **55**(6): 4901-4914. Available from:  
9 <https://doi.org/10.1029/2018WR024067>

10 Polson, D., Bollasina, M., Hegerl, G.C. & Wilcox, L.J. (2014) Decreased monsoon precipitation in the  
11 Northern Hemisphere due to anthropogenic aerosols. *Geophysical Research Letters*, **41**(16),  
12 6023-6029. Available from: <https://doi.org/10.1002/2014GL060811>

13 Rayner, N.A., Parker, D.E., Horton, E.B., Folland, C.K., Alexander, L.V., Rowell, D.P. et al. (2003)  
14 Global analyses of sea surface temperature, sea ice, and night marine air temperature since the late  
15 nineteenth century, *Journal of Geophysical Research: Atmospheres*, **108**, 4407. Available from:  
16 <https://doi.org/10.1029/2002JD002670>

17 Rotstayn, L.D., Collier, M.A., Chrastansky, A., Jeffrey, S.J., & Luo, J. (2013) Projected effects of  
18 declining aerosols in RCP4.5: unmasking global warming? *Atmospheric Chemistry and Physics*,  
19 **13**(7), 10883-10905. Available from: <https://doi.org/10.1029/2002JD002670>

20 Song, F., Zhou, T., & Qian, Y. (2014) Responses of East Asian summer monsoon to natural and  
21 anthropogenic forcings in the 17 latest CMIP5 models. *Geophysical Research Letters*, **41**, 596– 603.  
22 Available from: <https://doi.org/10.1002/joc.6887>

23 Stott, P.A., Christidis, N., Otto, F.E.L., Sun, Y., Vanderlinden, J.P., van Oldenborgh, G.J. et al. (2016)  
24 Attribution of extreme weather and climate-related events. *WIREs Climate Change*, **7**, 23-41.  
25 Available from: <https://doi.org/10.1002/wcc.380>

26 Sun, Q. & Miao, C. (2018) Extreme Rainfall (R20mm, RX5day) in Yangtze–Huai, China, in June–July  
27 2016: The Role of ENSO and Anthropogenic Climate Change. *Bulletin of the American*  
28 *Meteorological Society*, **99**(1), S102-S106. Available from:

1 <https://doi.org/10.1175/BAMS-D-17-0091.1>

2 Sun, Y., Dong, S.Y., Hu, T., Zhang, X. & Stott, P. (2019) Anthropogenic Influence on the Heaviest June  
3 Precipitation in Southeastern China since 1961. *Bulletin of the American Meteorological Society*,  
4 100(1), S79-S83. Available from: <https://doi.org/10.1175/BAMS-D-18-0114.1>

5 Sun, Y., Zhang, X., Ding, Y., Chen, D., Qin, D. & Zhai, P. (2021) Understanding human influence on  
6 climate change in China. *National Science Review*, **9**(3), 113. Available from:  
7 <https://doi.org/10.1093/nsr/nwab113>

8 Tang, H., Wang, Z., Tang, B., Ma, Y., Pei, L., Tian, F. et al. (2022) Reduced probability of 2020 June–July  
9 persistent heavy Meiyu rainfall event in the mid-lower reaches of the Yangtze River basin under  
10 anthropogenic forcing. *Bulletin of the American Meteorological Society*, **103**(1), S83-S89. Available  
11 from: <https://doi.org/https://doi.org/10.1175/BAMS-D-21-0167.1>

12 Tang, Y., Huang, A., Wu, P., Huang, D., Xue, D. & Wu, Y. (2021) Drivers of summer extreme  
13 precipitation events over East China. *Geophysical Research Letters*, **48**, e2021GL093670. Available  
14 from: <https://doi.org/10.1029/2021GL093670>

15 Tao, L., Hu, Y. & Liu, J. (2016) Anthropogenic forcing on the Hadley circulation in CMIP5 simulations.  
16 *Climate Dynamics*, **46**(9), 3337-3350. Available from: <https://doi.org/10.1007/s00382-015-2772-1>

17 Teutschbein, C. & Seibert, J. (2012) Bias correction of regional climate model simulations for  
18 hydrological climate-change impact studies: Review and evaluation of different methods. *Journal of*  
19 *Hydrology*, **456-457**, 12-29. Available from: <https://doi.org/10.1016/j.jhydrol.2012.05.052>

20 Tian, F., Dong, B., Robson, J. & Sutton, R. (2018) Forced decadal changes in the East Asian summer  
21 monsoon: the roles of greenhouse gases and anthropogenic aerosols. *Climate Dynamics*. **51**,  
22 3699–3715. Available from: <https://doi.org/10.1007/s00382-018-4105-7>

23 Vecchi, G.A., Soden, B.J., Wittenberg, A.T., Held, I.M., Leetmaa, A. & Harrison, M.J. (2006) Weakening  
24 of tropical Pacific atmospheric circulation due to anthropogenic forcing. *Nature*, **441**(7089), 73-76.  
25 Available from: <https://doi.org/10.1038/nature04744>

26 Wang, Y., Luo, Y. & Shafeeque, M. (2019) Using a Gaussian Function to Describe the Seasonal Courses  
27 of Monthly Precipitation and Potential Evapotranspiration across the Yellow River Basin, China.  
28 *Journal of Hydrometeorology*, **20**(11), 2185-2201. Available from:

1 <https://doi.org/https://doi.org/10.1175/JHM-D-19-0019.1>

2 Wang, Z. & Qian, Y. (2009) Frequency and intensity of extreme precipitation events in China (in Chinese).

3 *Advances in Water Science*, **20**(1), 1-9. Available from:

4 <https://doi.org/10.3321/j.issn:1001-6791.2009.01.001>

5 Wang, Z., Zhang, H. & Zhang, X. (2015) Simultaneous reductions in emissions of black carbon and  
6 co-emitted species will weaken the aerosol net cooling effect. *Atmospheric Chemistry and Physics*,

7 **15**(7), 3671-3685. Available from: <https://doi.org/10.5194/acp-15-3671-2015>

8 Wang, Z., Zeng, Z., Lai, C., Lin, W., Wu, X. & Chen, X. (2017) A regional frequency analysis of  
9 precipitation extremes in Mainland China with fuzzy c-means and L-moments approaches.

10 *International Journal of Climatology*, **37**, 429-444. Available from: <https://doi.org/10.1002/joc.5013>

11 Wang, Z., Sun, Y., Zhang, X., Li, T., Li, C., Min, S.-K. et al. (2023) Human influence on historical  
12 heaviest precipitation events in the Yangtze River Valley. *Environmental Research Letters*, **18**,

13 024044. Available from: <https://doi.org/10.1088/1748-9326/acb563>

14 Wu, Q.Y., Li, Q.Q., Ding, Y.H., Shen, X.Y., Zhao, M.C. & Zhu, Y.X. (2022) Asian summer monsoon  
15 responses to the change of land–sea thermodynamic contrast in a warming climate: CMIP6

16 projections. *Advances in Climate Change Research*, **13**(2), 205-217. Available from:

17 <https://doi.org/10.1016/j.accre.2022.01.001>.

18 Xu, H., Chen, H. & Wang, H. (2022) Detectable Human Influence on Changes in Precipitation Extremes  
19 Across China. *Earth's Future*, **10**, e2021EF002409. Available from:

20 <https://doi.org/10.1029/2021EF002409>

21 Xu, Y., Lamarque, J. & Sanderson, B. (2018) The importance of aerosol scenarios in projections of future  
22 heat extremes. *Climatic Change*, **146**(3), 393-406. Available from:

23 <https://doi.org/10.1007/s10584-015-1565-1>

24 Yang, L., Villarini, G., Smith, J.A., Tian, F. & Hu, H. (2013) Changes in seasonal maximum daily  
25 precipitation in China over the period 1961 -2006. *International Journal of Climatology*, **33**(7),

26 1646-1657. Available from: <https://doi.org/10.1002/joc.3539>

27 Yang, Y., Ren, L., Wu, M., Wang, H., Song, F., Leung, R. et al. (2022) Abrupt emissions reductions during  
28 COVID-19 contributed to record summer rainfall in China. *Nature Communications*. **13**, 95.

1 Available from: <https://doi.org/10.1038/s41467-022-28537-9>

2 Yuan, X., Wang, S. & Hu, Z. (2018) Do Climate Change and El Niño Increase the Likelihood of Yangtze  
3 River Extreme Rainfall? *Bulletin of the American Meteorological Society*, **99**(1), S113-S117.  
4 Available from: <https://doi.org/10.1175/BAMS-D-17-0089.1>

5 Zhang, L., Fu, T.M., Tian, H., Ma, Y., Chen, J.p., Tsai, T.C. et al. (2020) Anthropogenic aerosols  
6 significantly reduce mesoscale convective system occurrences and precipitation over Southern China  
7 in April. *Geophysical Research Letters*. **47**, e2019GL086204. Available from:  
8 <https://doi.org/10.1029/2019GL086204>

9 Zhang, Y., Wang, D. & Ren, X. (2008) Seasonal variation of the meridional wind in the temperate jet  
10 stream and its relationship to the Asian Monsoon. *Acta Meteorologica Sinica*, **24**, 446– 454.

11 Zhang, Q., Li, J., Singh, V.P. & Xu, C.Y. (2013) Copula-based Spatio-temporal patterns of precipitation  
12 extremes in China. *International Journal of Climatology*, **33**(5), 1140-1152. Available from:  
13 <https://doi.org/10.1002/joc.3499>

14 Zhang, W., Li, W., Zhu, L., Ma, Y., Yang, L., Lott, F.C. et al. (2020) Anthropogenic Influence on 2018  
15 Summer Persistent Heavy Rainfall in Central Western China. *Bulletin of the American  
16 Meteorological Society*, **101**(1), S65-S70. Available  
17 from:<https://doi.org/10.1175/BAMS-D-19-0147.1>

18 Zhao, A., Stevenson, D. & Bollasina, M. (2019) The role of anthropogenic aerosols in future precipitation  
19 extremes over the Asian Monsoon Region. *Climate Dynamics*, **52**, 6257-6278. Available from:  
20 <https://doi.org/10.1007/s00382-018-4514-7>

21 Zhao, C., Tie, X. & Lin, Y. (2006) A possible positive feedback of reduction of precipitation and increase  
22 in aerosols over eastern central China. *Geophysical Research Letters*. **33**, L11814. Available from:  
23 <https://doi.org/10.1029/2006GL025959>

24 Zhou, T., Yu, R., Zhang, J., Drange, H., Cassou, C., Deser, C. et al. (2009). Why the Western Pacific  
25 Subtropical High Has Extended Westward since the Late 1970s. *Journal of Climate*, **22**(8),  
26 2199-2215. Available from: <https://doi.org/10.1175/2008JCLI2527.1>

27 Zhou, C., Wang, K. & Qi, D. (2018) Attribution of the July 2016 Extreme Precipitation Event Over  
28 China's Wuhang. *Bulletin of the American Meteorological Society*, **99**(1), S107-S112. Available from:



1 <https://doi.org/10.1175/BAMS-D-17-0090.1>

2 Zhou, T., Ren, L. & Zhang, W. (2021) Anthropogenic influence on extreme Meiyu rainfall in 2020 and its

3 future risk. *Science China Earth Sciences*, **64**, 1633–1644. Available from:

4 <https://doi.org/10.1007/s11430-020-9771-8>